Front. Electr. Electron. Eng. 2012, 7(4): 427–437
DOI 10.1007/s11460-012-0198-7

RESEARCH ARTICLE

Suresh MIKKILI, A. K. PANDA

RTDS hardware implementation and simulation of SHAF for mitigation of harmonics using p-q control strategy with PI and fuzzy logic controllers

Abstract The main objective of this paper is to develop PI and fuzzy controllers to analyze the performance of instantaneous real active and reactive power (p-q) control strategy for extracting reference currents of shunt active filters (SHAFs) under balanced, unbalanced, and balanced non-sinusoidal conditions. When the supply voltages are balanced and sinusoidal, both controllers converge to the same compensation characteristics. However, if the supply voltages are distorted and/or unbalanced sinusoidal, these controllers result in different degrees of compensation in harmonics. The p-q control strategy with PI controller is unable to yield an adequate solution when source voltages are not ideal. Extensive simulations were carried out with balance, unbalanced, and non-sinusoidal conditions. Simulation results validate the superiority of fuzzy logic controller over PI controller. The three-phase four-wire SHAF system is also implemented on a real-time digital simulator (RTDS hardware) to further verify its effectiveness. The detailed simulation and RTDS hardware results are included.

Keywords harmonic compensation, shunt active filter (SHAF), p-q control strategy, PI controller, fuzzy logic controller, real-time digital simulator (RTDS hardware)

1 Introduction

Sinusoidal voltage is a conceptual quantity produced by an ideal alternating current (AC) generator built with finely distributed stator and field windings that operate in a uniform magnetic field. Since neither the winding distribution nor the magnetic field are uniform in a working AC machine, voltage waveform distortions are created, and the voltage-time relationship deviates from the pure sine function. The distortion at the point of generation is very small (about 1% to 2%), but nonetheless it exists. Since this is a deviation from a pure sine wave, the deviation is in the form of an episodic function, and by definition, the voltage distortion contains harmonics [1].

When a pure sinusoidal voltage is applied to a certain type of load, the current drawn by the load is proportional to the voltage and impedance and follows the envelope of the voltage waveform. These loads are referred to as linear loads (loads where the voltage and current follow one another without any distortion to their pure sine waves) [2]. Examples of linear loads are resistive heaters, incandescent lamps, and constant speed induction and synchronous motors. In contrast, some loads cause the current to vary disproportionately with the voltage during each half cycle. These loads are defined as nonlinear loads, and the current and voltage have waveforms that are no sinusoidal containing distortions, whereby the 50-Hz waveform has numerous additional waveforms superimposed upon it, creating multiple frequencies within the normal 50-Hz sine wave. The multiple frequencies are harmonics of the fundamental frequency. Examples of nonlinear loads are battery chargers, electronic ballasts, variable frequency drives, and switching mode power supplies.

As nonlinear currents flow through a facilities electrical system and the distribution-transmission lines, additional voltage distortions are produced due to the impedance associated with the electrical network. Thus, as electrical power is generated, distributed, and utilized, voltage and current waveform distortions are produced. It is noted that non-sinusoidal current results in many problems for the utility power supply company, such as low power factor, low energy efficiency, electromagnetic interference (EMI), distortion of line voltage, etc. Eminent issues always arise

Received March 21, 2011; accepted March 13, 2012

Suresh MIKKILI (✉), A. K. PANDA
Department of Electrical Engineering, National Institute of Technology, Rourkela, Orissa 769008, India
E-mail: msuresh.ee@gmail.com

in three-phase four-wire system; it is well known that zero line may be overheated or may cause fire disaster as a result of excessive harmonic current flowing through the neutral line, mostly triplen harmonics. Thus, a perfect compensator is necessary to avoid the consequences due to harmonics [3].

Although several control techniques and strategies have been developed but still the performance of filter is in contradiction, these became the primary motivation for the current paper. The present paper mainly focused on two controllers, i.e., fuzzy [4] and PI. Additionally, we have implemented a filter with instantaneous active and reactive power (p-q) method and analyzed the performance of filter under different main voltages. The simulation results confirm that fuzzy controller presents superior performance over PI controller. To validate current observations, real-time digital simulator (RTDS hardware) [5] results are included.

2 Compensation principle

The active power filter (APF) is controlled to draw/supply the compensating current [6] if from/to the load to cancel out the current harmonics on AC side and reactive power flow from/to the source, thereby making the source current in phase with source voltage.

Figure 1 shows the basic compensation principle of the active power filter and it serves as an energy storage element to supply the real power difference between load and source during the transient period. When the load condition changes the real power balance between the mains and the load will be disturbed. This real power difference is to be compensated by the direct current (DC) capacitor. This changes the DC capacitor voltage away from the reference voltage.

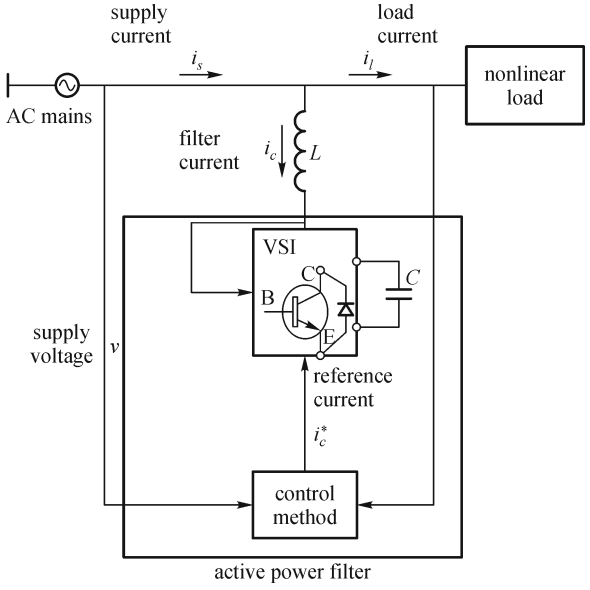

Fig. 1 Basic compensation principle

To keep satisfactory operation or the active filter, the peak value of the reference source current must be adjusted to proportionally change the real power [7] drawn from the source. This real power charged/discharged by the capacitor compensates the real power difference between the power consumed by the load and that supplied by the source. If the DC capacitor voltage is recovered and attains the reference voltage, the real power supplied by the source is supposed to be equal to that consumed by the load again. In this fashion, the peak value of the reference source current can be obtained by regulating the average voltage of the DC capacitor.

3 Instantaneous real active and reactive power (p-q) control strategy

Instantaneous real active and reactive power theory (Fig. 2) (or p-q theory) was first proposed by Akagi and co-authors in 1984 [1] and has since been the subject of various interpretations and improvements. In this method [8], a set of voltages (v_a, v_b, v_c) and currents (i_a, i_b, i_c) from phase coordinates are first transferred to the $0\alpha\beta$ coordinates using Clark transformation:

$$\begin{bmatrix} v_0 \\ v_\alpha \\ v_\beta \end{bmatrix} = C \begin{bmatrix} v_a \\ v_b \\ v_c \end{bmatrix}, \quad \begin{bmatrix} i_0 \\ i_\alpha \\ i_\beta \end{bmatrix} = C \begin{bmatrix} i_{La} \\ i_{Lb} \\ i_{Lc} \end{bmatrix}, \tag{1}$$

$$C = \sqrt{\frac{2}{3}} \begin{bmatrix} \frac{1}{\sqrt{2}} & \frac{1}{\sqrt{2}} & \frac{1}{\sqrt{2}} \\ 1 & -\frac{1}{2} & -\frac{1}{2} \\ 0 & \frac{\sqrt{3}}{2} & -\frac{\sqrt{3}}{2} \end{bmatrix}. \tag{2}$$

The p-q formulation defines the generalized instantaneous power, $p(t)$, and instantaneous reactive power vector, $q(t)$ [9], in terms of the α-β-0 components as

$$p = v_{\alpha\beta 0} \cdot i_{\alpha\beta 0} = v_\alpha i_\alpha + v_\beta i_\beta + v_0 i_0, \tag{3}$$

$$q = v_{\alpha\beta 0} \times i_{\alpha\beta 0} = \begin{bmatrix} q_\alpha \\ q_\beta \\ q_0 \end{bmatrix} = \begin{bmatrix} \begin{vmatrix} v_0 & v_\alpha \\ i_0 & i_\alpha \end{vmatrix} \\ \begin{vmatrix} v_a & v_\beta \\ i_a & i_\beta \end{vmatrix} \\ \begin{vmatrix} v_\beta & v_0 \\ i_\beta & i_0 \end{vmatrix} \end{bmatrix}, \tag{4}$$

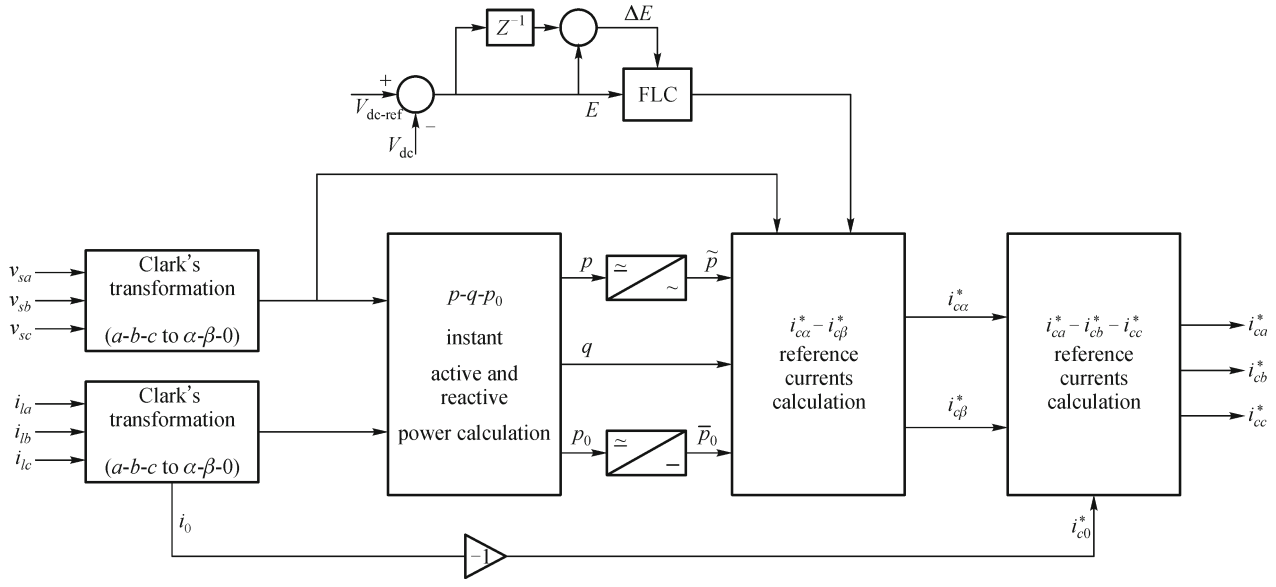

Fig. 2 Control method for shunt current compensation based on p-q theory

$$q = \left\|\vec{q}\right\| = \sqrt{q_\alpha^2 + q_\beta^2 + q_0^2}, \tag{5}$$

$$\begin{bmatrix} i_\alpha \\ i_\beta \\ i_0 \end{bmatrix} = \frac{1}{v_{\alpha\beta 0}^2} \begin{bmatrix} v_\alpha & 0 & v_0 & -v_\beta \\ v_\beta & -v_0 & 0 & v_\alpha \\ v_0 & v_\beta & -v_\alpha & 0 \end{bmatrix} \begin{bmatrix} p \\ q_\alpha \\ q_\beta \\ q_0 \end{bmatrix}, \tag{6}$$

where $v_{\alpha\beta 0}^2 = v_\alpha^2 + v_\beta^2 + v_0^2$.

The reference source current in the $\alpha\beta 0$ frame is

$$\begin{bmatrix} i_{s\alpha} \\ i_{s\beta} \\ i_{s0} \end{bmatrix} = \frac{1}{v_{\alpha\beta 0}^2} \begin{bmatrix} v_\alpha & 0 & v_0 & -v_\beta \\ v_\beta & -v_0 & 0 & v_\alpha \\ v_0 & v_\beta & -v_\alpha & 0 \end{bmatrix} \begin{bmatrix} p \\ q_\alpha \\ q_\beta \\ q_0 \end{bmatrix}. \tag{7}$$

The objective of the p-q strategy [10] is to get the source to give only the constant active power demanded by the load $p_s(t) = p_{L0}(t) + p_{L\alpha\beta}(t)$. In addition, the source must deliver no zero-sequence active power $i_{s0\text{-ref}} = 0$ (so that the zero-sequence component of the voltage at the point of common coupling (PCC) does not contribute to the source power). The reference source current in the α-β-0 frame is therefore

$$\begin{bmatrix} i_{s\alpha\text{-ref}} \\ i_{s\beta\text{-ref}} \\ i_{s0\text{-ref}} \end{bmatrix} = \frac{\overline{p_{L\alpha\beta}} + \overline{p_{L0}}}{v_\alpha^2 + v_\beta^2} \begin{bmatrix} v_\alpha \\ v_\beta \\ 0 \end{bmatrix}. \tag{8}$$

4 Construction of PI controller

Figure 3 shows the internal structure of the control circuit. The control scheme consists of PI controller, limiter, and three-phase sine wave generator for reference current generation and generation of switching signals. The peak value of reference currents is estimated by regulating the DC link voltage. The actual capacitor voltage is compared with a set reference value [11]. The error signal is then processed through a PI controller, which contributes to zero steady error in tracking the reference current signal.

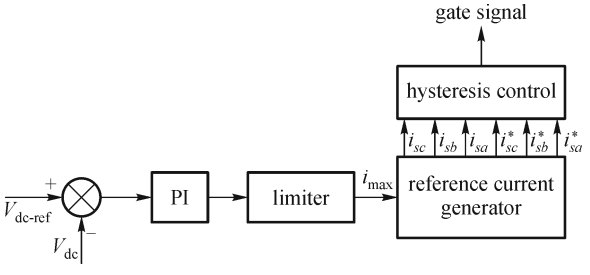

Fig. 3 Conventional PI controller

The output of the PI controller is considered as peak value of the supply current (i_{max}), which is composed of two components: a) fundamental active power component of load current and b) loss component of APF to maintain the average capacitor voltage to a constant value. Peak value of the current (i_{max}) so obtained is multiplied by the unit sine vectors in phase with the respective source

voltages to obtain the reference compensating currents. These estimated reference currents (i^*_{sa}, i^*_{sb}, i^*_{sc}) and sensed actual currents (i_{sa}, i_{sb}, i_{sc}) are compared at a hysteresis band, which gives the error signal for the modulation technique. This error signal decides the operation of the converter switches. In this current control circuit configuration, the source/supply currents i_{sabc} are made to follow the sinusoidal reference current i_{abc} within a fixed hysteretic band. The width of hysteresis window determines the source current pattern, its harmonic spectrum, and the switching frequency of the devices. The DC link capacitor voltage [12] is kept constant throughout the operating range of the converter. In this scheme, each phase of the converter is controlled independently. To increase the current of a particular phase, the lower switch of the converter associated with that particular phase is turned on while to decrease the current the upper switch of the respective converter phase is turned on. With this, one can realize the potential and feasibility of PI controller.

• Hysteresis current controller

The actual source currents are monitored instantaneously and then compared to the reference currents [5] generated by the proposed algorithm. To get accurate instantaneous control, switching of IGBT device should be such that the error signal should approach to zero and thus provide quick response. For this reason, hysteresis current controller with fixed band, which derives the switching signals of three-phase IGBT-based VSI bridge, is used. The upper device and the lower device in one phase leg of VSI are switched in complementary manner; else, a dead short circuit will take place. The APF reference currents i^*_{sa}, i^*_{sb}, i^*_{sc} compared with sensed source currents i_{sa}, i_{sb}, i_{sc} and the error signals are operated by the hysteresis current controller to generate the firing pulses that activate the inverter power switches in a manner that reduces the current error.

5 Construction of fuzzy logic controller

Figure 4 shows the fuzzy inference system (FIS) [5]. It consists of

- FIS editor,
- Membership function editor,
- Rule editor,
- Rule viewer, and
- Surface viewer.

The FIS editor handles the high-level issues for the system: How many inputs and output variables? What are their names? The membership function editor is used to define the shapes of all the membership functions associated with each variable. The rule editor is for editing the list of rules that define the behavior of the system. The rule viewer and the surface viewer are used for looking at, as opposed to editing, the FIS. They are strictly read-only tools. Used as a diagnostic, it can show which rules are active or how individual membership function shapes are influencing the results. The surface viewer is used to display the dependency of one of the outputs on any one or two of the inputs, that is, it generates and plots an output surface map for the system.

- The FIS editor, the membership function editor, and the rule editor can all read and modify the FIS data, but the rule viewer and the surface viewer do not modify anything in the FIS data.
- One of the key issues in all fuzzy sets is how to determine fuzzy membership functions.
- The membership function fully defines the fuzzy set.
- A membership function provides a measure of the degree of similarity of an element to a fuzzy set.
- Membership functions can take any form, but there are some common examples that appear in real applications.
- Membership functions can either be chosen by the user arbitrarily based on the user's experience (membership function chosen by two users could be different depending upon their experiences, perspectives, etc.) or be designed using machine learning methods (e.g., artificial neural networks, genetic algorithms, etc.).
- There are different shapes of membership functions: triangular, trapezoidal, piecewise linear, Gaussian, bell-shaped, etc.

5.1 Defuzzification

For defuzzification, the centroid of area (COA) method was considered:

$$\mu_A(x) = \text{defuzz}(x,mf,type),$$

where defuzz(x, mf, $type$) returns a defuzzified value out of a membership function mf positioned at associated variable value x, using one of several defuzzification [12] strategies according to the argument type. The variable type can be one of the following:

- centroid: centroid of area,
- bisector: bisector of area,
- mom: mean value of maximum,
- som: smallest (absolute) value of maximum, or
- lom: largest (absolute) value of maximum.

5.2 Design of control rules

The fuzzy control rule [12] design involves defining rules that relate the input variables to the output model properties. As fuzzy logic controller is independent of system model, the design is mainly based on the intuitive

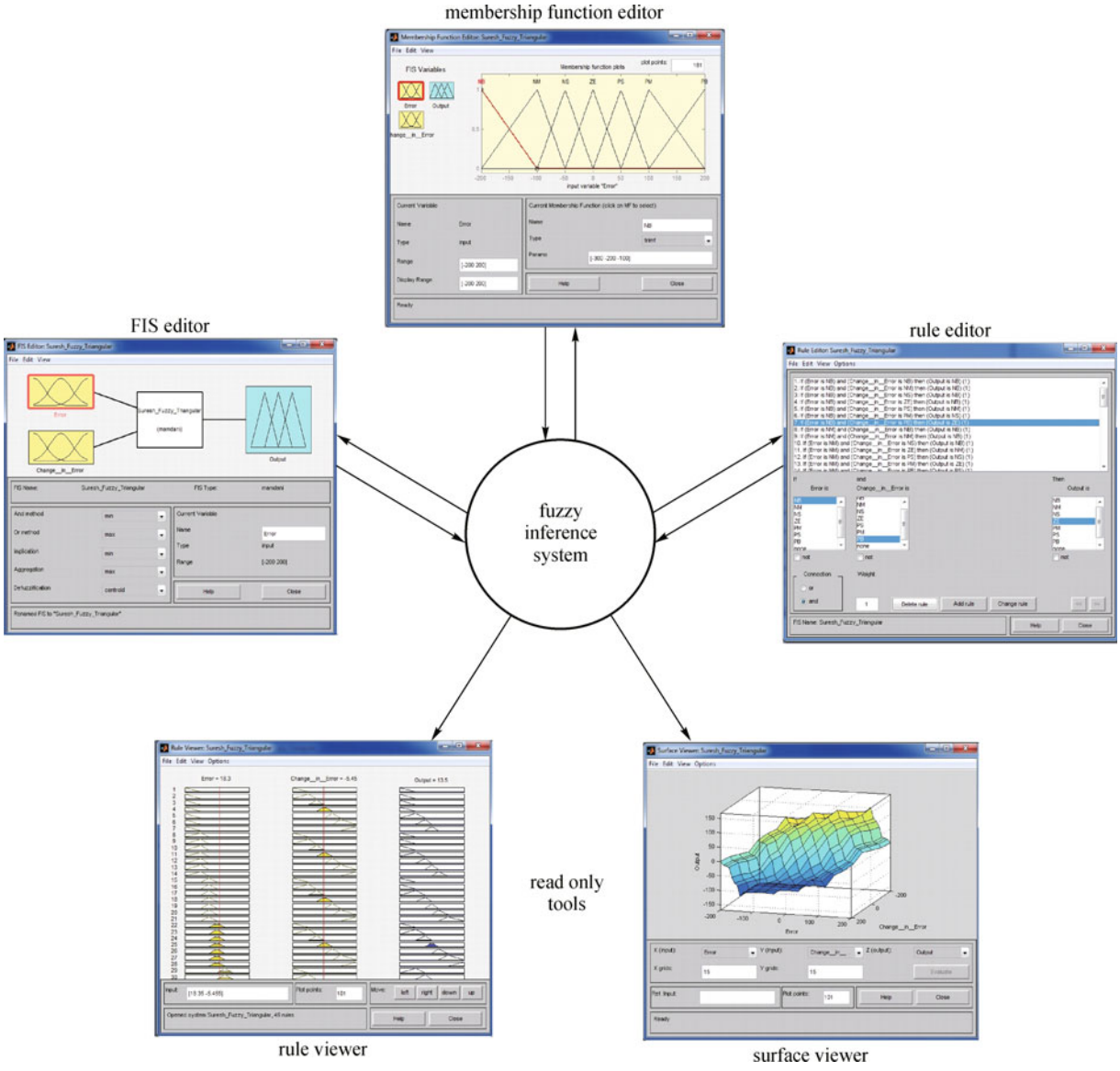

Fig. 4 Fuzzy inference system with triangular membership function

feeling for, and experience of, the process. The rules are expressed in English like language with syntax such as If {error E is X and change of error ΔE is Y} then {control output is Z}. For better control performance, finer fuzzy petitioned subspaces {NB (negative big), NM (negative medium), NS (negative small), ZE (zero), PS (positive small), PM (positive medium), and PB (positive big)} are used and summarized in Table 1. These seven membership functions are same for input and output and characterized using triangular membership function [13], as can be seen in Fig. 5.

6 RTDS hardware

This simulator was developed with the aim of meeting the transient simulation needs of electromechanical drives and electric systems while solving the limitations of traditional real-time simulators, as shown in Fig. 6. It is based on a central principle: the use of widely available, user-friendly, highly competitive commercial products (PC platform, Simulink™). The real-time simulator [5] consists of two main tools: a) a real-time distributed simulation package (RT-LABORATORY) for the execution of Simulink block

Table 1 Rule base

E	ΔE						
	NB	NM	NS	ZE	PS	PM	PB
NB	NB	NB	NB	NB	NM	NS	ZE
NM	NB	NB	NB	NM	NS	ZE	PS
NS	NB	NB	NM	NS	ZE	PS	PM
ZE	NB	NM	NS	ZE	PS	PM	PB
PS	NM	NS	ZE	PS	PM	PB	PB
PM	NS	ZE	PS	PM	PB	PB	PB
PB	ZE	PS	PM	PB	PB	PB	PB

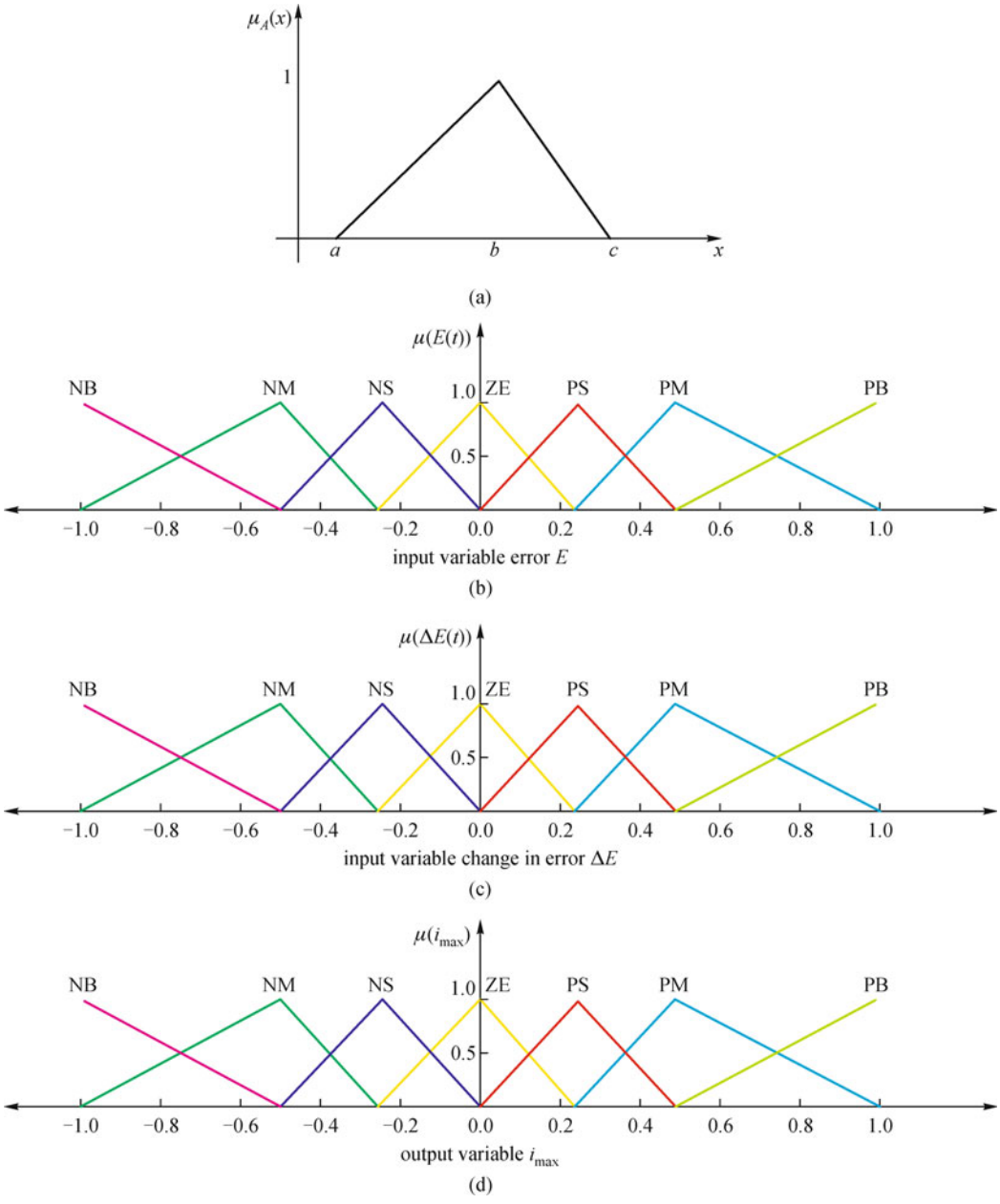

Fig. 5 (a) Triangular membership function; (b) input variable error E (triangular membership function); (c) input change in error (normalized triangular membership function); (d) output i_{max} (normalized triangular membership function)

diagrams on a PC-cluster and b) algorithmic toolboxes designed for the fixed-time-step simulation of stiff electric circuits and their controllers. Real-time simulation and hardware-in-the-loop (HIL) applications are increasingly recognized as essential tools for engineering design and especially in power electronics and electrical systems.

The RTDS hardware used in the implementation of the RTDS is modular, hence making it possible to size the processing power to the simulation tasks at hand. Figure 6 demonstrates typical hardware configurations. The OP5142 (Fig. 7) is one of the key building blocks in the modular OP5000 I/O system from Opal-RT Technologies. It allows the incorporation of FPGA technologies in RT-LABORATORY simulation clusters for distributed execution of HDL functions and high-speed, high-density digital I/O in real-time models. Based on the highest density Xilinx Spartan-3 FPGAs, the OP5142 can be attached to the backplane of an I/O module of either a Wanda 3U- or Wanda 4U-based Opal-RT simulation system. It communicates with the target PC via a PCI-Express ultra-low-latency real-time bus interface. As can be seen, the simulator can take on several forms including a new portable version that can be easily transported to a power plant or substation for on-site pre-commissioning tests.

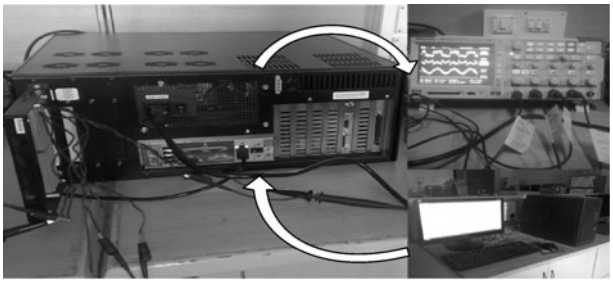

Fig. 6 RTDS hardware

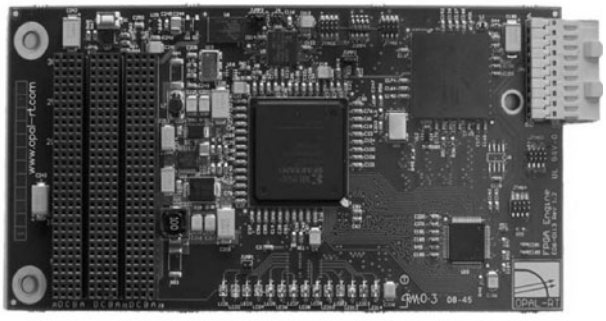

Fig. 7 OP5142 layout and connectors

7 Simulation and RTDS hardware results

Figures 8–10 illustrate the performance of shunt active power filter under different main voltages, as load is highly inductive; current drawn by the load is integrated with rich harmonics.

Figure 8 illustrates the performance of shunt active power filter under balanced sinusoidal voltage condition. Total harmonic distortion (THD) for p-q method with PI controller using Matlab simulation is 2.15% and using RTDS hardware is 2.21%; THD for p-q method with fuzzy controller using Matlab simulation is 1.27% and using RTDS hardware is 1.45%.

Figure 9 illustrates the performance of shunt active power filter under unbalanced sinusoidal voltage condition, THD for p-q method with PI controller using Matlab simulation is 4.16% and using RTDS hardware is 4.23%; THD for p-q method with fuzzy controller using Matlab simulation is 2.98% and using RTDS hardware is 3.27%.

Figure 10 illustrates the performance of shunt active power filter under balanced non-sinusoidal voltage condition, THD for p-q method with PI controller using Matlab simulation is 5.31% and using RTDS hardware is 5.41%; THD for p-q method with fuzzy controller using Matlab simulation is 3.85% and using RTDS hardware is 4.15%.

Figure 11 gives the THD comparison of p-q control strategy with PI and fuzzy controllers using Matlab/Simulink and RTDS hardware.

8 Conclusion

In the present paper, two controllers are developed and verified with three-phase four-wire system. Although two controllers are capable to compensate current harmonics in the three-phase four-wire system, it is observed that fuzzy logic controller shows better dynamic performance over conventional PI controller. Pulse width modulation (PWM) pattern generation based on carrier less hysteresis-based current control is used for quick response. It is also observed that DC voltage regulation system valid to be a stable and steady-state error free system was obtained. Thus, with fuzzy logic and p-q approach, a novel SHAF can be developed. The three-phase four-wire SHAF system is also implemented on an RTDS hardware to further verify its effectiveness. Essential simulation and RTDS hardware results are presented to validate the performance of SHAF.

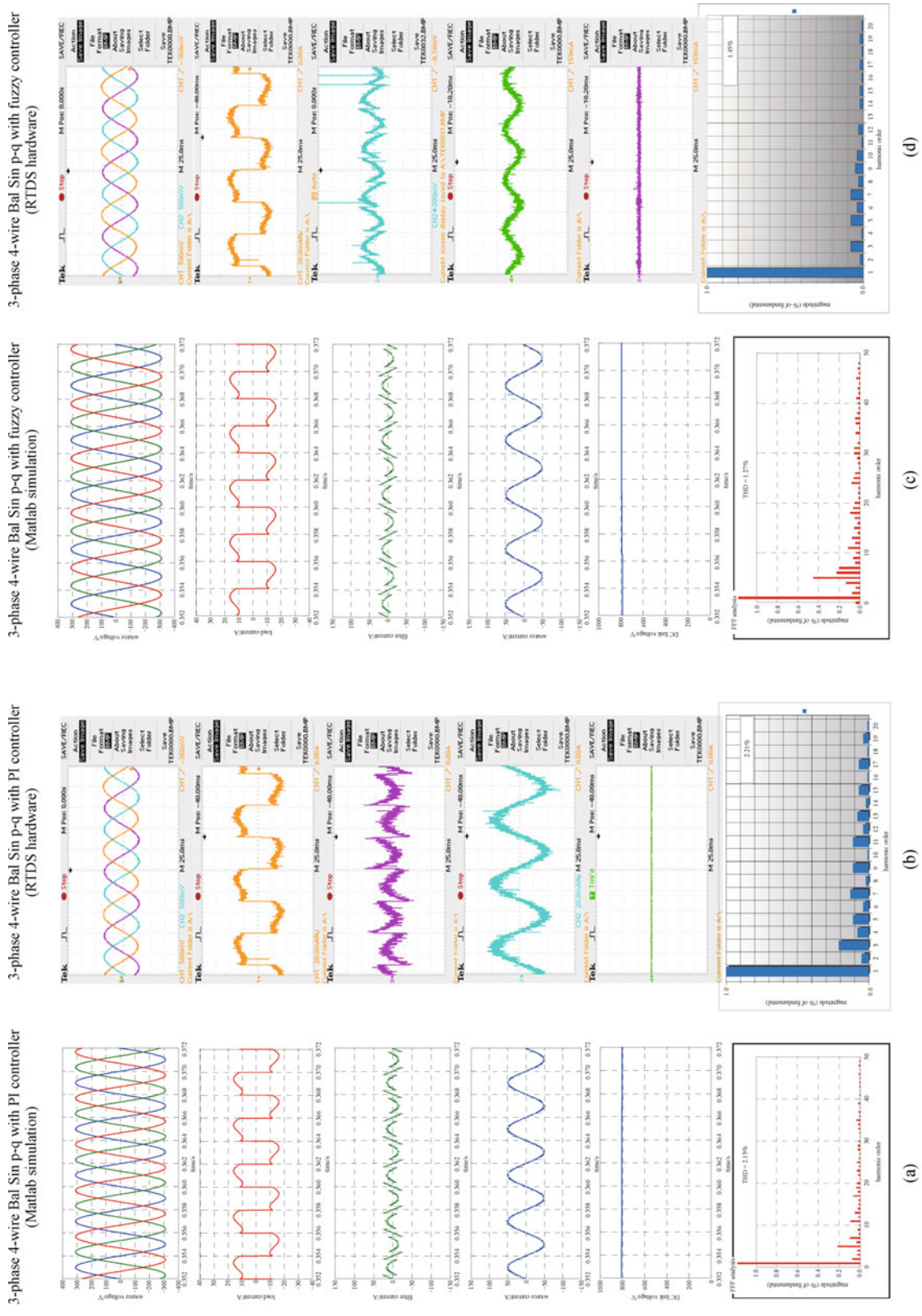

Fig. 8 Three-phase four-wire shunt active filter response with p-q control strategy under balanced (Bal) sinusoidal (Sin) using (a) PI with Matlab, (b) PI with RTDS hardware, (c) fuzzy with Matlab, and (d) fuzzy with RTDS hardware

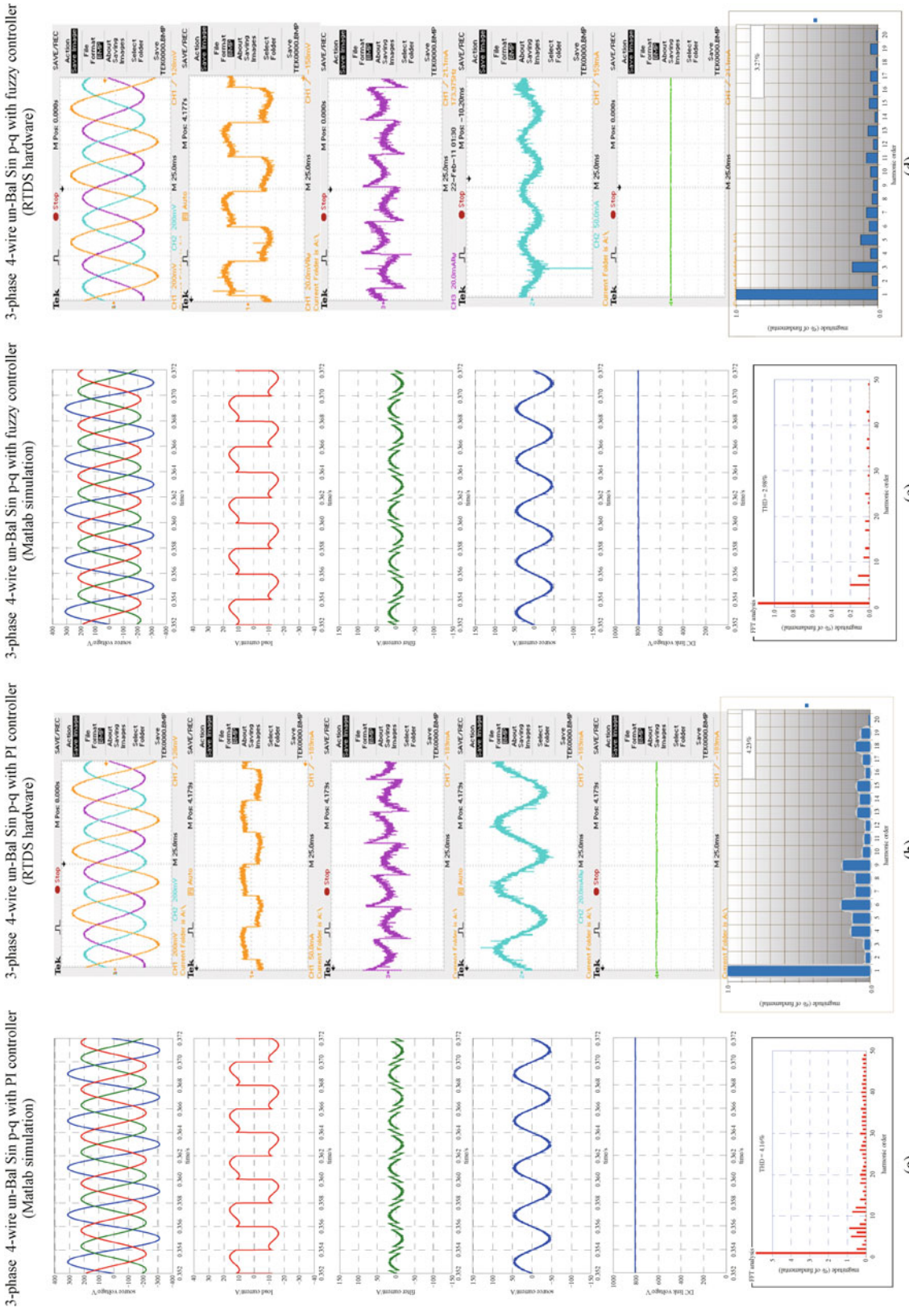

Fig. 9 Three-phase four-wire shunt active filter response with p-q control strategy under unbalanced (un-Bal) sinusoidal (Sin) using (a) PI with Matlab, (b) PI with RTDS hardware, (c) fuzzy with Matlab, and (d) fuzzy with RTDS hardware

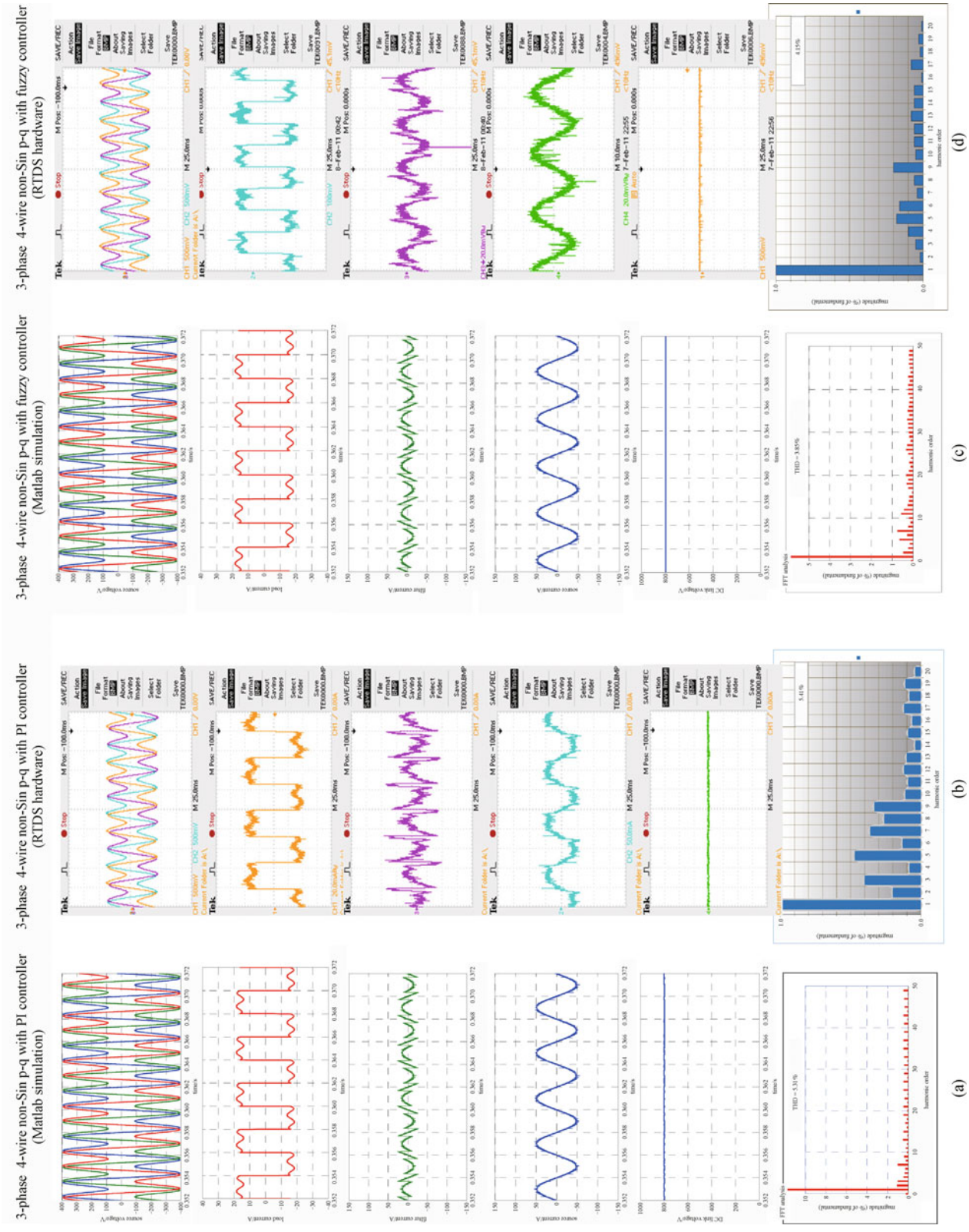

Fig. 10 Three-phase four-wire shunt active filter response with p-q control strategy under non-sinusoidal (non-Sin) using (a) PI with Matlab, (b) PI with RTDS hardware, (c) fuzzy with Matlab, and (b) fuzzy with RTDS hardware

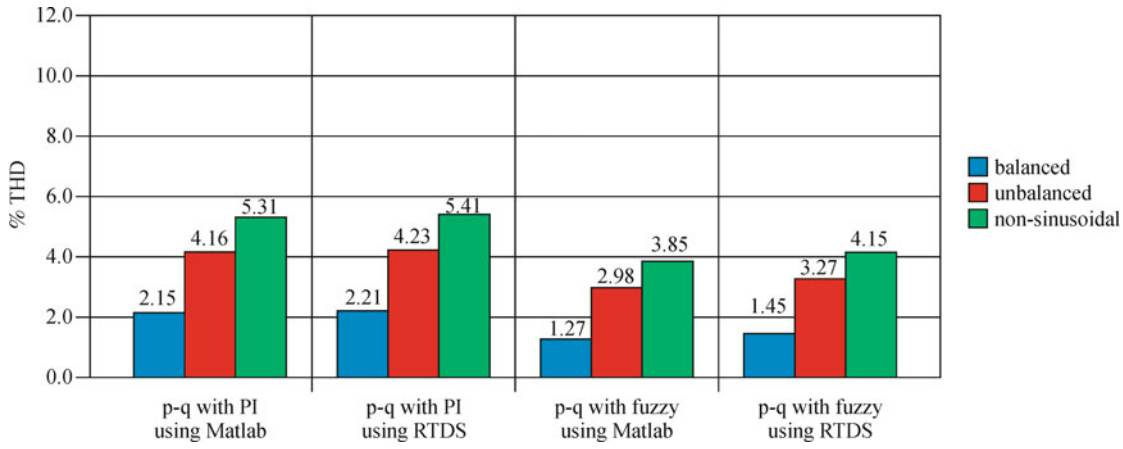

Fig. 11 THD for p-q control strategy with PI and fuzzy controller using Matlab and RTDS hardware

References

1. Akagi H, Kanazawa Y, Nabae A. Instantaneous reactive power compensators comprising switching devices without energy storage components. IEEE Transactions on Industry Applications, 1984, IA-20(3): 625–630
2. Gyugyi L, Strycula E C. Active AC power filters. In: Proceedings of IEEE/IAS Annual Meeting. 1976, 529–535
3. Mikkili S, Panda A K. PI and fuzzy logic controller based 3-phase 4-wire shunt active filters for the mitigation of current harmonics with the I_d-I_q control strategy. Journal of power Electronics, 2011, 11(6): 914–921
4. Akagi H. New trends in active filters for power conditioning. IEEE Transactions on Industry Applications, 1996, 32(6): 1312–1322
5. Mikkili S, Panda A K. Fuzzy logic controller based 3-ph 4-wire SHAF for current harmonics compensation with I_d-I_q control strategy using simulation and RTDS hardware. In: Proceedings of the Ninth IEEE International Conference on Power Electronics and Drive Systems. 2011, 430–435
6. Akagi H, Watanabe E H, Aredes M. Instantaneous Power Theory and Applications to Power Conditioning. New Jersey: IEEE Press/ Wiley Interscience, 2007
7. Peng F Z, Ott G W Jr, Adams D J. Harmonic and reactive power compensation based on the generalized instantaneous reactive power theory for three-phase four-wire systems. IEEE Transactions on Power Electronics, 1998, 13(6): 1174–1181
8. Montero M I M, Cadaval E R, Gonzalez F B. Comparison of control strategies for shunt active power filters in three-phase four-wire systems. IEEE Transactions on Power Electronics, 2007, 22(1): 229–236
9. Aredes M, Hafner J, Heumann K. Three-phase four-wire shunt active filter control strategies. IEEE Transactions on Power Electronics, 1997, 12(2): 311–318
10. Rodriguez P, Candela J I, Luna A, Asiminoaei L, Teodorescu R, Blaabjerg F. Current harmonics cancellation in three-phase four-wire systems by using a four-branch star filtering topology. IEEE Transactions on Power Electronics, 2009, 24(8): 1939–1950
11. Salmeron P, Herrera R S. Distorted and unbalanced systems compensation within instantaneous reactive power framework. IEEE Transactions on Power Delivery, 2006, 21(3): 1655–1662
12. Kirawanich P, O'Connell R M. Fuzzy logic control of an active power line conditioner. IEEE Transactions on Power Electronics, 2004, 19(6): 1574–1585
13. Jain S K, Agrawal P, Gupta H O. Fuzzy logic controlled shunt active power filter for power quality improvement. IEE Proceedings — Electric Power Applications, 2002, 149(5): 317–328